Impact of acrylamide on postnatal developmental changes in the cerebellum of albino rat offspring and the potential ameliorative effects of nanohydroxyapatite and vitamin B12

Zamzam Nasrallah Abdel-Moaty[a], Rana A. Ali[b], Rasha M.AbdelFattah[c], Ahmed Talaat Galal[d], Safa El-Nahas[e], Basma Tito Abd elhameed[f], Yahia A. Amin[g*], Maha Abd-El Baki Ahmed[a]

[a]Department of Human Anatomy & Embryology, Faculty of Medicine, South Valley University, Qena, Egypt.
[b]Department of physiology, Faculty of Science, South Valley University, Qena, Egypt.
[c]Department of Human Anatomy & Embryology, Faculty of Medicine, Sohag University, Sohag, Egypt.
[d]Department of Human Anatomy & Embryology, Faculty of Medicine, Assiut University, Assiut, Egypt.
[e]Department of Chemistry, Faculty of Science, South Valley University, Qena, Egypt
fDepartment of Pathology, Faculty of Medicine, South Valley University, Qena, Egypt.
[g]Department of Theriogenology, Faculty of Veterinary Medicine, Aswan University, Aswan 81528, Egypt

Abstract

Background: Acrylamide (ACR) causes neurotoxicity and fetal damage due to its placental transfer. Therefore, protective treatment is required.

Objectives: This study aims to evaluate the neurotoxic effects of ACR exposure in pregnant and nursing rats on the cerebellum of their offspring at postnatal days (PND) 15 and 21. Additionally, investigation of the potential protective effects of administering Nano-hydroxyapatite (NHA) and vitamin B12 (Vit.B12) in combination with ACR to the mothers against ACR-induced cerebellum damage in the offspring was performed.

Materials and methods: 40 pregnant females' rats were divided into four groups (10 for each): control, acrylamide (10mg/kg), acrylamide+nano-hydroxyapatite (300 mg/kg), and acrylamide+Vit.B12 (1mg/kg), with treatments administered for 5 weeks. Male produced offspring were sacrificed at postnatal days 15 and 21. Cerebellar tissues were collected for histopathology and electron microscopy investigations, while tissue samples were collected for oxidant/antioxidant markers such as malondialdehyde (MDA), superoxide dismutase (SOD), catalase (CAT), and glutathione peroxidase (GP_X) analysis using standard colorimetric assays.

DOI: 10.21608/SVUIJM.2025.409665.2229
***Correspondence**: yahiaamin2030@gmail.com
Received: 4 August,2025.
Revised: 13 August, 2025.
Accepted: 25 August, 2025.
Published: 29 August, 2025
Cite this article as Zamzam Nasrallah Abdel-Moaty, Rana A. Ali, Rasha M.AbdelFattah, Ahmed Talaat Galal, Safa El-Nahas, Basma Tito Abd elhameed, Yahia A. Amin[g*], Maha Abd-El Baki Ahmed. (2025). Impact of acrylamide on postnatal developmental changes in the cerebellum of albino rat offspring and the potential ameliorative effects of nanohydroxyapatite and vitamin B12. Vol.8, Issue 2, pp: 415-439.

Results: Acrylamide significantly reduced Purkinje cell count (P=0.0001), as well as the thickness of the granular, Purkinje, and molecular layers (P=0.0001). Administration of NHA and ViT.B12, in combination with ACR preserved Purkinje cells, and both treatments improved layer thickness (P<0.05). Acrylamide reduced CAT, SOD, GPX activities (all P<0.0001), and increased MDA levels (P<0.0001). Vitamin B12 significantly restored enzyme activities and normalized MDA levels (P=0.1652). Nano-hydroxyapatite improved all parameters but was less effective than Vit.B12.

Conclusion: Acrylamide induces cerebellar damage and oxidative stress in the offspring. Nano-hydroxyapatite provides partial protection, while Vit.B12 offered superior neuroprotection, significantly restoring structural, histopathological and oxidant/antioxidant markers.

Keywords: Acrylamide; Neurotoxicity; Hydroxyapatite; Vitamin B12; Albino rats offspring.

Introduction

Acrylamide (ACR) is an industrial chemical used in wastewater treatment and/or mining, and is also present in tobacco smoke. It is formed during the high-temperature cooking of carbohydrate-rich foods such as chips, cakes, and bread through the Maillard reaction-a non-enzymatic interaction between reducing sugars and amino acids or proteins **(Zhao et al., 2022).** ACR has been linked to carcinogenicity, neurotoxicity, and reproductive toxicity. In animals, repeated exposure to ACR in doses ranging from 0.5 to 50 mg/kg/day induces neurological disorders by covalently binding to cysteine residues in presynaptic neuronal proteins, thereby impairing neurotransmission. ACR also causes neuronal injury via oxidative stress and inflammatory mechanisms **(Zhao et al., 2022; Yan et al., 2023).** Human exposure has been associated with ataxia, muscle weakness, unsteady gait, and impaired motor control, indicating potential damage to both cerebral and cerebellar regions. ACR water solubility allows it and its metabolites to cross the placenta and accumulate in fetal tissues, heightening concern over its developmental toxicity **(Peivasteh-Roudsari et al., 2024).**

Hydroxyapatite (HA), a naturally occurring form of calcium phosphate and a major component of bone, is well known for its high biocompatibility, making it especially suitable for bone repair applications. Its crystal lattice permits substitution of calcium ions with other metal ions such as ions of Ba, Sr, Cd, Pb, Zn, and Cu, giving it potential for heavy metal detoxification **(Zia et al., 2022).** Upon implantation, HA undergoes ion exchange with body fluids, releasing calcium and phosphate ions that may enter circulation and influence central nervous system function **(Awais et al., 2022; Kubiak-Mihkelsoo et al., 2025).** Nanotechnology represents a major advancement in various areas of medical treatment, including antimicrobial therapy **(Amin et al. 2023a)**, toxicity mitigation, and the enhancement of therapeutic drug combinations. One notable form of nanotechnology is nano-hydroxyapatite (n-HA). Notably, the nano form is called nano-hydroxyapatite (n-HA)-has shown neuroprotective effects by lowering lipid peroxidation, reducing apoptotic cell death, accelerating DNA repair, and enhancing neurotransmitter synthesis **(Abbas et al., 2019).** Additionally, n-HA reduces the amplitude and frequency of excitatory postsynaptic currents (EPSCs), thereby modulating synaptic transmission and

promoting nerve recovery **(Liu et al., 2012).**

Vitamin B12 (cobalamin), a water-soluble vitamin found in eggs, milk, fish, and meat, plays an essential role in neuronal health. It functions as a coenzyme in metabolic pathways critical for red blood cell production and central nervous system integrity **(Calderón-Ospina et al., 2020; Mathew et al., 2024).** Vitamin B12 protects neurons by mitigating the oxidative stress, reducing inflammation, and enhancing neuronal repair mechanisms **(Ehmedah, 2024).** It also preserves the myelin sheath, supports remyelination, and facilitates nerve regeneration through cellular repair and structural renewal **(Baltrusch, 2021).**

This study aims to evaluate the neurotoxic effects of acrylamide (ACR) exposure in pregnant and nursing rats on the cerebellum of their offspring at postnatal days 15 and 21. Additionally, it investigates the potential protective effects of administering nano-hydroxyapatite (HA) and vitamin B12, in combination with ACR, to the mothers against ACR-induced cerebellar damage in the offspring.

Materials and methods

Experimental animals

The study protocol was approved by the Institutional Research Committee at the Faculty of Medicine, South Valley University, Qena, Egypt with the approval number of SVU MD ANA0012234616. Forty adult albino female rats and 20 adult male albino rats weighing 180-250 g were obtained. The study was carried out at the animal house of the Faculty of Medicine, South Valley University. Throughout the study, rats were housed in wire mesh cages under strict hygienic measures and was allowed to acclimatize for two weeks before the start of the experiment. Rats were kept in room temperature, 55-60% humidity and normal light/dark cycle with free access to food pellets and tap water.

Mating and detection of pregnancy

For mating, each group of three females was housed with one male overnight. Pregnancy was confirmed the next morning by the presence of sperm in vaginal smears or a visible vaginal plug, which was considered gestational day 0 **(Ognio et al., 2003).** The 40 pregnant females were randomly allocated into four experimental groups (n = 10 each). Ten male offspring of each group were later randomly subdivided into two subgroups based on postnatal day (PND) of sacrifice: PND15 and PND21.The animals were sacrified and transcardially perfused with physiological saline.

Experimental design

The current study was conducted on male offspring obtained from pregnant rats, which were divided into four equal groups (10 in each group). Group I (control group) included offspring from healthy female albino rats that were fed a standard diet and administered physiological saline without any additional treatment. Group II (Acrylamide group) included offspring from pregnant rats that received oral administration of acrylamide at a dosage of 10 mg/kg body weight once daily, starting from the 7th day of gestation and continuing up to 21 days after delivery (a total of 5 weeks). Acrylamide, in powdered form (125 grams), was obtained from El Gomhoria Company, Assiut, Egypt, following the methodology established by **Moawad et al. (2019).** Group III (acrylamide + Nano-hydroxyapatite) included offspring from pregnant rats that received a combined treatment of acrylamide and nano-hydroxyapatite. Female rats were administered acrylamide (10 mg/kg/day) alongside nano-hydroxyapatite (300 mg/kg), both

delivered via oral gavage for five weeks, similar to Group II. The treatment protocol followed the methodologies described by **Hafez et al. (2012) and Malla et al. (2024)**.The nano-hydroxyapatite utilized in this group was manufactured by a precipitation method **(El-Nahas S.et al., 2022). Group IV** (Acrylamide + Vitamin B12) included offspring from pregnant rats that received a combined treatment of acrylamide and vitamin B12. Female rats in this group were administered acrylamide (10 mg/kg/day) along with vitamin B12 (1 mg/kg/day), both given orally for five weeks. Vitamin B12 was obtained in powdered form (25 grams) from El Gomhoria Company, Assiut, Egypt, following the dosage protocol outlined by **Moosavirad et al. (2016).** All chemical reagents used in the experiment were of analytical grade and confirmed to be of high purity.

Tissue homogenate preparation

Tissue samples were collected from each offspring at the postnatal days 15 and 21. Immediately after euthanasia and cerebellum extraction, the cerebellar tissue homogenate was prepared, according to **Behairy et al., (2020)**. In the cold phosphate-buffered saline (PBS, 0.01 mol/L, pH 7), the cerebellar tissue was homogenized using the glass homogenizer (1:9 W/V). The resulting homogenates will be centrifuged for 5 min at 5000× g; the supernatants will be filtered with a Millipore filter (0.45 µm) to eliminate tissue debris.

At the end of the experiment, animals were fasted overnight and anesthetized using diethyl ether inhalation**(Aguwa et al., 2020)**. After confirming deep anesthesia, the animals were euthanized by decapitation in accordance with approved ethical guidelines. Subsequently, the skull was opened, and the brain was carefully dissected. The heads were dissected for obtaining the cerebellar biopsies. Adherent tissues were removed, and the brains were immersed in 10% neutral buffered formalin for histopathological analysis (light and electron microscopy), **(Fig.1)** shows the summarized study design.

All procedures were performed in accordance with the institutional guidelines for animal care and use**.**

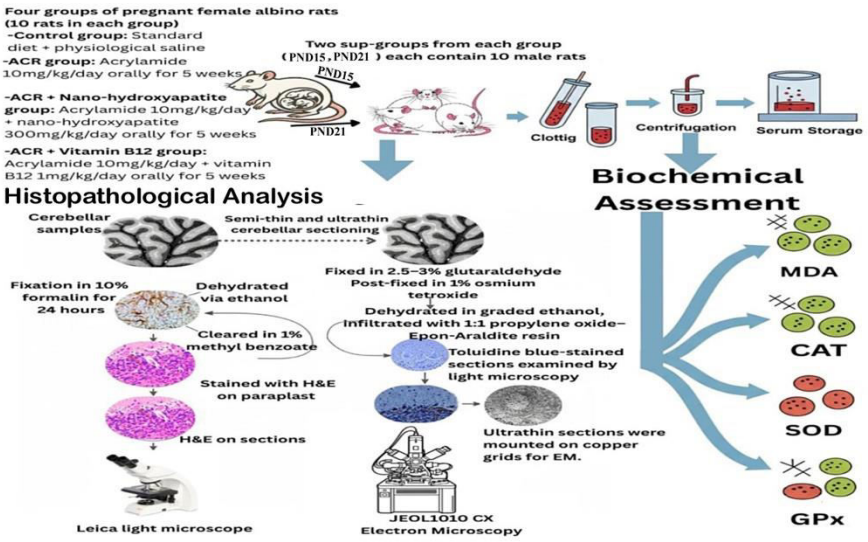

Fig.1. Study design.

Oxidant/antioxidant profile assessment

Malondialdehyde (MDA) levels were determined colorimetrically using commercial kits provided by Biodiagnostic (Cat.No: MD 25 28) and based on the thiobarbituric acid (TBA) reaction as described by **Ruiz-Larnea et al. (1994).** Absorbance was measured at 535 nm and MDA concentration was calculated as the following equation: MDA (nmol/g tissue) = (Sample / Standard) × (10 / g tissue). Catalase (CAT) activity was measured according to **Aebi (1984)** using Biodiagnostic kits (Cat.No: CA 25 17), with absorbance measured spectrophotometrically and enzyme activity was calculated as: CAT (U/g) = (Standard – Sample) / Standard × (1 / g tissue). Superoxide dismutase (SOD) activity was assessed using Biodiagnostic kits (Cat.No: SD 25 21) according to the method of **Nishikimi et al. (1972)**. Enzymatic activity was calculated using the formula: SOD (U/g tissue) = % inhibition × 3.75 × (1 / g tissue). Glutathione peroxidase (GPx) activity was evaluated using the method of **De Paglia and Valentine (1967)** with Biodiagnostic kits (Cat.No: GP 25 24). Absorbance was measured at 340 nm, and GPx activity was calculated using the following equation: GPx (U/g tissue) = (ΔA340/min) / 0.00622 × 121.

Light microscopy assessment

For light microscopy, histopathological examination followed the protocol of **Bancroft and Gamble (2008).** Cerebellar samples were fixed in 10% neutral buffered formalin for 24 hours, dehydrated through graded ethanol concentrations, cleared in 1% methyl benzoate, and embedded in paraplast after impregnation. Sections were stained with hematoxylin and eosin (H&E) and examined using a Leica microscope (CH9435Heerbrugg, Leica Microsystems, Switzerland).

Electron microscopy assessment

For electron microscopy, semi-thin and ultrathin sectioning was carried out based on the methodology by **Ayache et al. (2010).** Cerebellar tissues were sagittally divided, and small blocks were fixed in 2.5-3% glutaraldehyde in sodium cacodylate buffer for 24 hours. Post-fixation was done using 1% osmium tetroxide for two hours. Dehydration was achieved using graded ethanol, followed by infiltration with a 1:1 mixture of propylene oxide and Epon-Araldite resin. Semi-thin sections were stained with toluidine blue and examined under light microscopy. Ultrathin sections (~50 nm) were mounted on copper grids for transmission electron microscopy and analyzed using a JEOL1010 CX (Japan) at South Valley University.

Morphometric analysis

The purkinje cells count and thickness of granular, purkinje and molecular layers were measured (**Celik et al., 2018)** at the postnatal days 15 and 21 of the studied groups (at magnification of 200).

Statistical analysis

Data were analyzed using SPSS 26, expressing qualitative data as numbers/percentages and quantitative data as mean ± SD. Central tendency was measured by the mean, dispersion by SD. Group comparisons used ANOVA to test for significant differences among three or more groups, with significance set at $p< 0.05$.

Results

Preparation and Characterization of Nano-HAP

(Fig.2) implies the nanohydroxyapatite sample that was fabricated this manner, along with various characteristics such as XRD, SEM,and TEM examination, which

validated the validity of this substance**.**

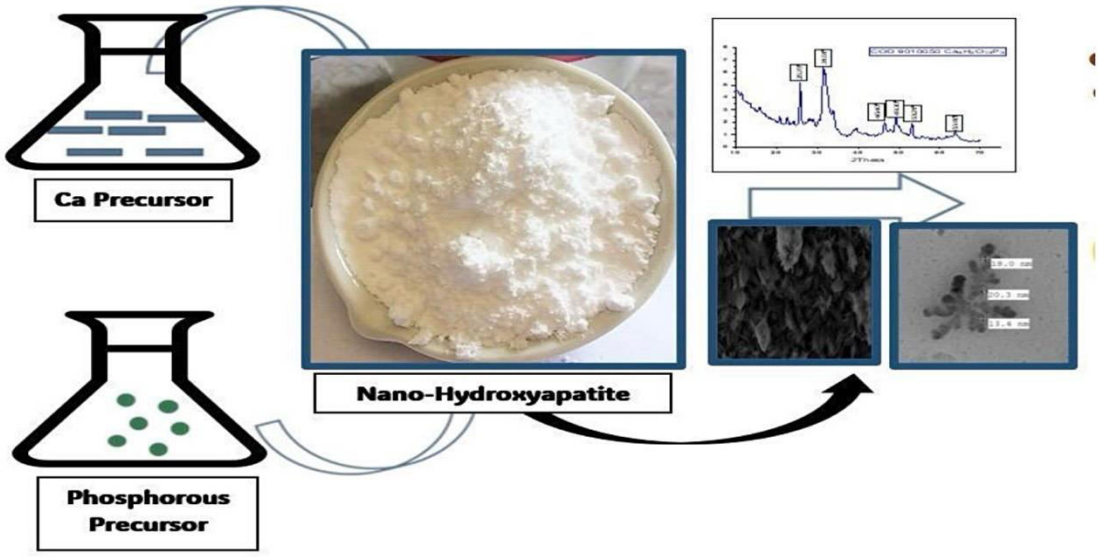

Fig.2. TEM photomicrograph of the nanoparticles

Results of the statistical analysis of the histopathological investigation

Table.1 and Fig.3 showed the statistical analysis of the histopathological alterations on the cerebellum of the produced offspring of the four studied group (15 days postnatal). Histopathological investigation revealed that all studied parameter was significantly reduced in the ACR group compared with the control one such as Purkinje cells count (10 ± 1.2 vs. 15.2 ± 1.1, $P < 0.0001$), granular layer thickness (100.3 ± 1.1 vs. 104.1 ± 1.2, $P < 0.0001$), Purkinje layer thickness (17.87 ± 0.84 vs. 28.14 ± 0.46, $P < 0.0001$), and molecular layer thickness (77 ± 1.3 vs. 80.9 ± 1.5, $P < 0.0001$).

Nano-hydroxyapatite co-treatment significantly increased the values of the histopathological studied parameter compared to the ACR group as the following: Purkinje cells count (13 ± 0.9, $P = 0.0006$), Purkinje layer thickness (20.81 ± 0.41, $P = 0.0006$), granular layer thickness (101.3 ± 0.54, $P < 0.0001$), and molecular layer thickness (78 ± 0.2, $P < 0.0001$). However, values remained significantly lower than control for most parameters ($P < 0.0001$).

Vitamin B12 co-treatment significantly restored Purkinje cells count (14 ± 1.3, $P = 0.1024$ vs. control, but $P < 0.0001$ vs. acrylamide), Purkinje layer thickness (24.81 ± 0.44, $P < 0.0001$ vs. acrylamide), granular layer (103.3 ± 0.6, $P = 0.0836$ vs. control, $P < 0.0001$ vs. acrylamide), and molecular layer thickness (79 ± 0.65, $P = 0.1626$ vs. control, $P < 0.0001$ vs. acrylamide).

Vitamin B12 showed greater recovery across most layers compared to nano-hydroxyapatite, particularly in Purkinje and granular layers. However, molecular layer improvement was comparable between both agents.

Table 1. Statistical analysis of cerebellar histopathological findings in 15-day-old offspring from four groups of pregnant rats

Variables	Offspring of control group	Offspring of acrylamide treated mothers group	Offspring of acrylamide + nano-hydroxyapatite treated mothers group	Offspring of acrylamide + vitamin B12 treated mothers group	*P. Value*
Purkinje cells count	15.2 ± 1.1	10 ± 1.2	13 ± 0.9	14 ± 1.3	*< 0.0001**
	P1 < 0.0001*, P2 = 0.0006*, P3 = 0.1024, P4 < 0.0001*, P5 < 0.0001*, P6 = 0.2179				
Granular layer thickness	104.1 ± 1.2	100.3 ± 1.1	101.3 ± 0.54	103.3 ± 0.6	*< 0.0001**
	P1 < 0.0001*, P2 < 0.0001*, P3 = 0.2185, P4 = 0.0836, P5 < 0.0001*, P6 = 0.0001*				
Purkinje layer thickness	28.14 ± 0.46	17.87 ± 0.84	20.81 ± 0.41	24.81 ± 0.44	*< 0.0001**
	P1<0.0001*, P2 = 0.0006*, P3<0.0001*, P4 < 0.0001*, P5 < 0.0001*, P6 < 0.0001**				
Molecular layer thickness	80.9 ± 1.5	77 ± 1.3	78 ± 0.2	79 ± 0.65	*< 0.0001**
	P1 < 0.0001*, P2 < 0.0001*, P3 = 0.0014*, P4 = 0.1626, P5 = 0.0008*, P6 = 0.1626				

P1 = offspring control vs. offspring of acrylamide treated mothers, P2 = offspring control vs. offspring of acrylamide + nano-hydroxyapatite treated mothers , P3 = offspring control vs. offspring of acrylamide + vitamin B12 treated mothers, P4 = offspring of acrylamide treated mothers vs. Offspring of acrylamide + nano-hydroxyapatite treated mothers, P5 = offspring of acrylamide treated mothers vs. offspring of acrylamide + vitamin B12 treated mothers, P6 = Offspring of acrylamide + nano-hydroxyapatite treated mothers vs. offspring of acrylamide + vitamin B12 treated mothers.

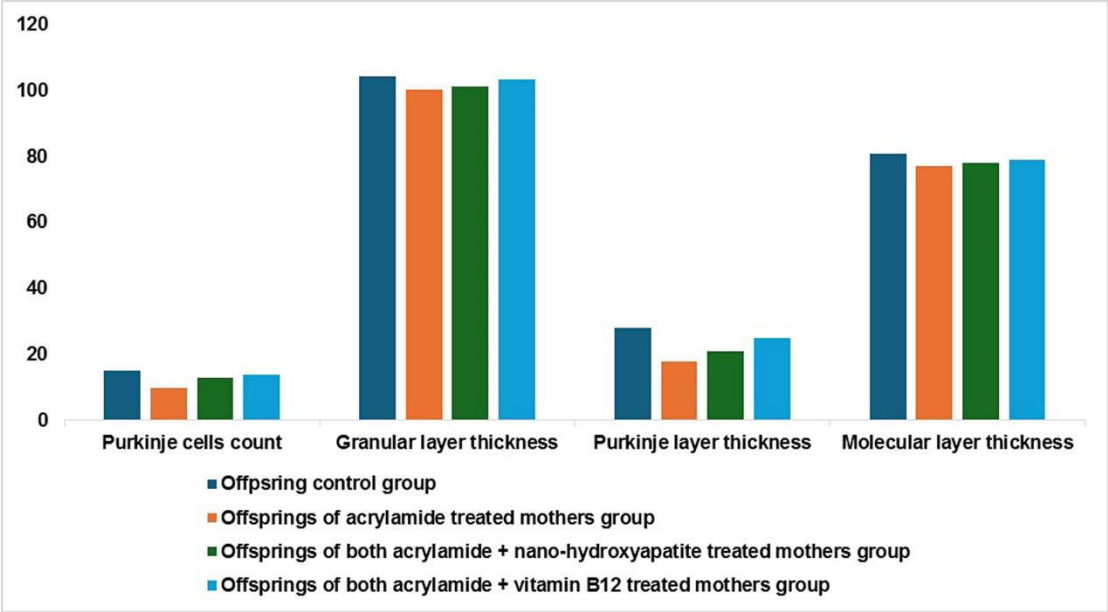

Fig.3. Statistical analysis of cerebellar histopathological findings in 15-day-old offspring from four groups of pregnant rats

Table.2 and Fig.4 showed the statistical analysis of the histopathological alterations on the cerebellum of the produced offspring of the four studied group (21 days postnatal). At day 21, acrylamide group showed significant decrease of the Purkinje cells count (7.8 ± 1.6), granular layer thickness (130.6 ± 3.1), Purkinje layer thickness (19.32 ± 0.74), and molecular layer thickness (132.3 ± 1.6) compared to the control group (P < 0.0001).

Nano-hydroxyapatite co-treatment with ACR significantly increased Purkinje cells count (9.4 ± 0.68, P = 0.0072), granular layer thickness (132.1 ± 0.09, P = 0.0005),

and Purkinje layer thickness (22.08 ± 0.57, P = 0.0006), but remained lower than control.

Vitamin B12 co-treatment with ACR significantly restored Purkinje cells count (10.2 ± 0.15, P = 0.001), granular layer thickness (135.3 ± 3.1, P = 0.0008), and Purkinje layer thickness (26.71 ± 0.75, P < 0.0001), with no significant difference from control in most parameters. Molecular layer thickness (134.3 ± 0.76) was preserved in both treated groups (P = 0.6575 vs. control). Vitamin B12 showed superior neuroprotection compared to nano-hydroxyapatite.

Table 2. Statistical analysis of cerebellar histopathological findings in 21-day-old offspring from four groups of pregnant rats

Variables	Offspring of control group	Offspring of acrylamide treated mothers group	Offspring of acrylamide + nano-hydroxyapatite treated mothers group	Offspring of acrylamide + vitamin B12 treated mothers group	*P. Value*
Purkinje cells count	11.4 ± 1.9	7.8 ± 1.6	9.4 ± 0.68	10.2 ± 0.15	*0.0001**
	P1 = 0.0001*, P2 = 0.0072*, P3 = 0.1789, P4 = 0.0415*, P5 = 0.001*, P6 = 0.5155				
Granular layer thickness	137 ± 2.3	130.6 ± 3.1	132.1 ± 0.09	135.3 ± 3.1	*0.0001**
	P1 = 0.0001*, P2 = 0.0005*, P3 = 0.4276, P4 = 0.5352, P5 = 0.0008*, P6 = 0.0315*				
Purkinje layer thickness	29.23 ± 0.6	19.32 ± 0.74	22.08 ± 0.57	26.71 ± 0.75	*0.0001**
	P1 < 0.0001*, P2 = 0.0006*, P3 < 0.0001*, P4 < 0.0001*, P5 < 0.0001*, P6 <0.0001*				
Molecular layer thickness	135.0 ± 1.9	132.3 ± 1.6	134.3 ± 0.76	134.3 ± 0.76	*0.0006**
	P1 = 0.0004*, P2 = 0.6575, P3 = 0.6575, P4 = 0.0111*, P5 = 0.0111*, P6 = 0.99				

P1 = offspring control vs offspring of acrylamide treated mothers , P2 = offspring control vs offspring of acrylamide + nano-hydroxyapatite treated mothers , P3 = offspring control vs offspring of acrylamide + vitamin B12 treated mothers, P4 = offspring of acrylamide treated mothers vs Offspring of acrylamide + nano-hydroxyapatite treated mothers, P5 = offspring of acrylamide treated mothers vs offspring of acrylamide + vitamin B12 treated mothers, P6 = Offspring of acrylamide + nano-hydroxyapatite treated mothers vs offspring of acrylamide + vitamin B12 treated mothers.

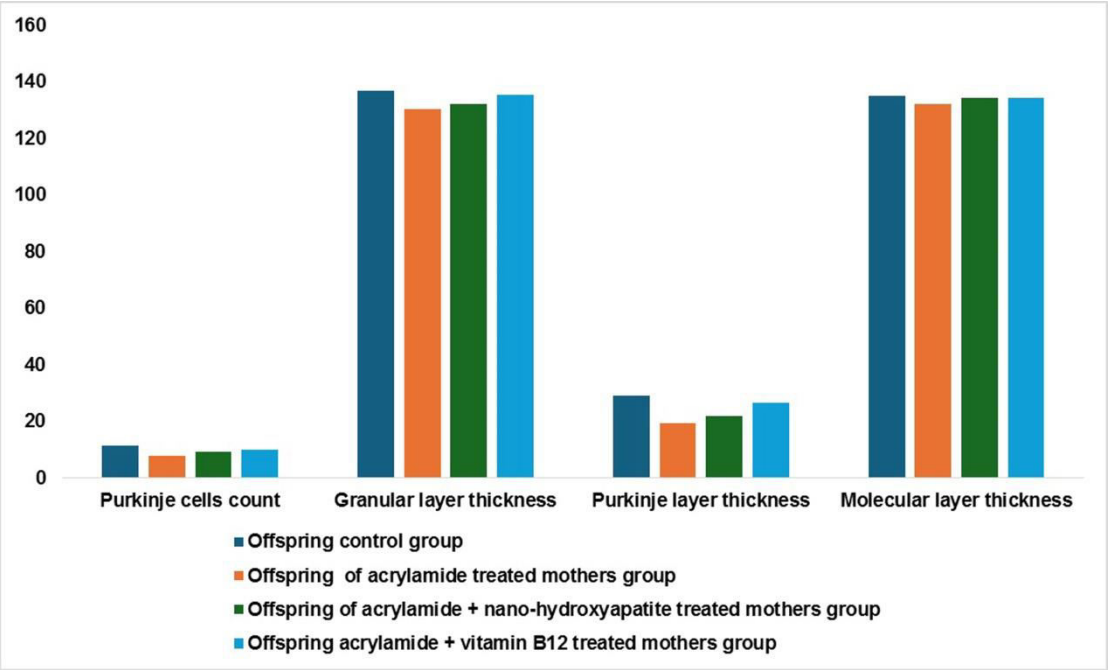

Fig.4. Statistical analysis of cerebellar histopathological findings in 21-day-old offspring from four groups of pregnant rats.

Oxidant/antioxidant results

Table.3 and Fig.5 showed the oxidant/antioxidant results of the produced offspring of the four studied group (15 days postnatal). Acrylamide group showed significant decrease in the levels of the CAT, SOD, and GPX activities ($P < 0.0001$), and elevated MDA levels ($P < 0.0001$), indicating marked oxidative stress. The two of combination of ACR with Nano-hydroxyapatite and/or vitamin B12 displayed significant improvement of all parameters versus the acrylamide group. Vitamin B12 co-treatment with ACR showed stronger effects on restoring CAT ($P < 0.0001$), SOD ($P < 0.0001$), GP_X ($P = 0.0004$), and reducing MDA ($P < 0.0001$), approaching control levels. Nano-hydroxyapatite co-treatment with ACR also showed significant improvements of CAT and MDA ($P < 0.0001$), SOD ($P = 0.0007$), and GP_X ($P = 0.0007$).

Table 3: Variation in oxidant/antioxidant biomarkers in 15-day-old offspring from control and treated groups of pregnant rats

Variables	Offspring control group	Offspring of Acrylamide treated mothers group	Offspring of acrylamide + nano-hydroxyapatite treated mothers group	Offspring of acrylamide + vitamin B12 treated mothers group	*P. Value*
CAT	16.04 ± 0.94	6.52 ± 0.27	8.58 ± 0.41	12.26 ± 0.29	*< 0.0001**
	P1 < 0.0001*, P2 < 0.0001*, P3 < 0.0001*, P4 < 0.0001*, P5 < 0.0001*, P6 < 0.0001*				
MDA	338.58 ± 5.63	578.39 ± 5.08	469.13 ± 13.77	362.21 ± 8.11	*< 0.0001**
	P1 < 0.0001*, P2 < 0.0001*, P3 < 0.0001*, P4 < 0.0001*, P5 < 0.0001*, P6 < 0.0001*				
SOD	129.41 ± 5.75	60.67 ± 5.22	78.58 ± 3.43	113.8 ± 4.98	*< 0.0001**
	P1 < 0.0001*, P2 < 0.0001*, P3 = 0.0007*, P4 < 0.0001*, P5 < 0.0001*, P6 < 0.0001*				
GP_X	458.71 ± 12.46	219.57 ± 4.69	361.71 ± 3.57	381.3 ± 4.04	*< 0.0001**
	P1 < 0.0001*, P2 < 0.0001*, P3 = 0.0007*, P4 < 0.0001*, P5 < 0.0001*, P6 = 0.0004*				

P1 = offspring control vs offspring of acrylamide treated mothers , P2 = offspring control vs offspring of acrylamide + nano-hydroxyapatite treated mothers , P3 = offspring control vs offspring of acrylamide + vitamin B12 treated mothers, P4 = offspring of acrylamide treated mothers vs Offspring of acrylamide + nano-hydroxyapatite treated mothers, P5 = offspring of acrylamide treated mothers vs offspring of acrylamide + vitamin B12 treated mothers, P6 = Offspring of acrylamide + nano-hydroxyapatite treated mothers vs offspring of acrylamide + vitamin B12 treated mothers. CAT: Catalase; MDA: Malondialdehyde; SOD: Superoxide dismutase; GPx: Glutathione peroxidase

Table.4 and Fig.6 showed the oxidant/antioxidant results of the produced offspring of the four studied group (21 days postnatal). Acrylamide significantly reduced CAT ($P < 0.0001$), SOD ($P < 0.0001$), and GP_X activities ($P < 0.0001$), and increased MDA levels ($P < 0.0001$), indicating oxidative stress. Nano-hydroxyapatite administration with ACR significantly improved CAT ($P = 0.0006$), SOD, GP_X, and MDA ($P < 0.0001$). Vitamin B12 administration with ACR showed superior restoration of the CAT ($P = 0.0004$), SOD, GP_X, and normalized MDA levels, with no significant difference from the control ($P = 0.1652$).

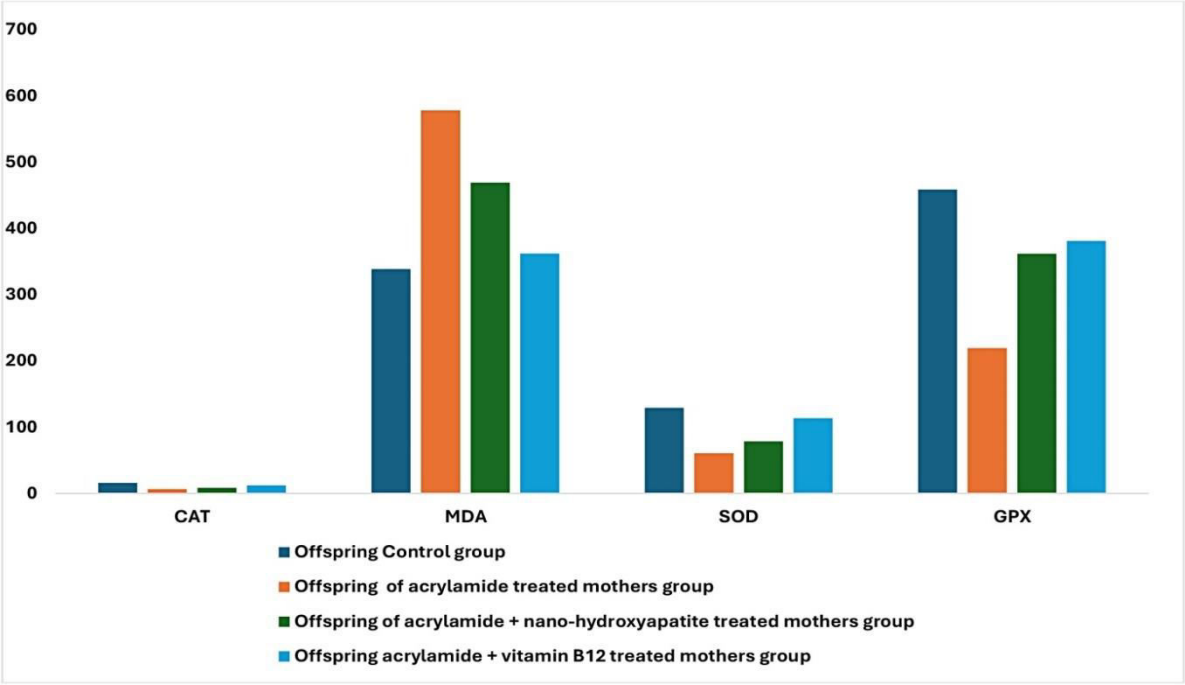

Fig.5. Variation in oxidant/antioxidant biomarkers in 15-day-old offspring from control and treated groups of pregnant rats

Table 4. Variation in oxidant/antioxidant biomarkers in 21-day-old offspring from control and treated groups of pregnant rats

Variables	Offspring control group	Offspring of Acrylamide treated mothers group	Offspring of acrylamide + nano-hydroxyapatite treated mothers group	Offspring of acrylamide + vitamin B12 treated mothers group	*P. Value*
CAT	20.24 ± 1.64	8.39 ± 0.75	11.33 ± 0.54	17.06 ± 0.62	*< 0.0001**
	P1 < 0.0001*, P2 < 0.0001*, P3 = 0.0006*, P4 < 0.0017*, P5 < 0.0001*, P6 = 0.0004*				
MDA	307.57 ± 5.1	547.07 ± 5.03	419.29 ± 30.77	328.5 ± 11.6	*< 0.0001**
	P1 < 0.0001*, P2 < 0.0001*, P3 = 0.1652, P4 < 0.0001*, P5 < 0.0001*, P6 = 0.0001*				
SOD	170.13 ± 4.4	77.87 ± 7.63	101.05 ± 3.59	146.43 ± 6.04	*< 0.0001**
	P1 < 0.0001*, P2 < 0.0001*, P3 < 0.0001*, P4 < 0.0001*, P5 < 0.0001*, P6 < 0.0001*				
GPX	640.57 ± 6.61	309.13 ± 5.31	511.34 ± 4.91	538.71 ± 5.75	*< 0.0001**
	P1 < 0.0001*, P2 < 0.0001*, P3 < 0.0001*, P4 < 0.0001*, P5 < 0.0001*, P6 < 0.0001*				

P1 = offspring control vs offspring of acrylamide treated mothers , P2 = offspring control vs offspring of acrylamide + nano-hydroxyapatite treated mothers , P3 = offspring control vs offspring of acrylamide + vitamin B12 treated mothers, P4 = offspring of acrylamide treated mothers vs Offspring of acrylamide + nano-hydroxyapatite treated mothers, P5 = offspring of acrylamide treated mothers vs offspring of acrylamide + vitamin B12 treated mothers, P6 = Offspring of acrylamide + nano-hydroxyapatite treated mothers vs offspring of acrylamide + vitamin B12 treated mothers. CAT: Catalase; MDA: Malondialdehyde; SOD: Superoxide dismutase; GPx: Glutathione peroxidase

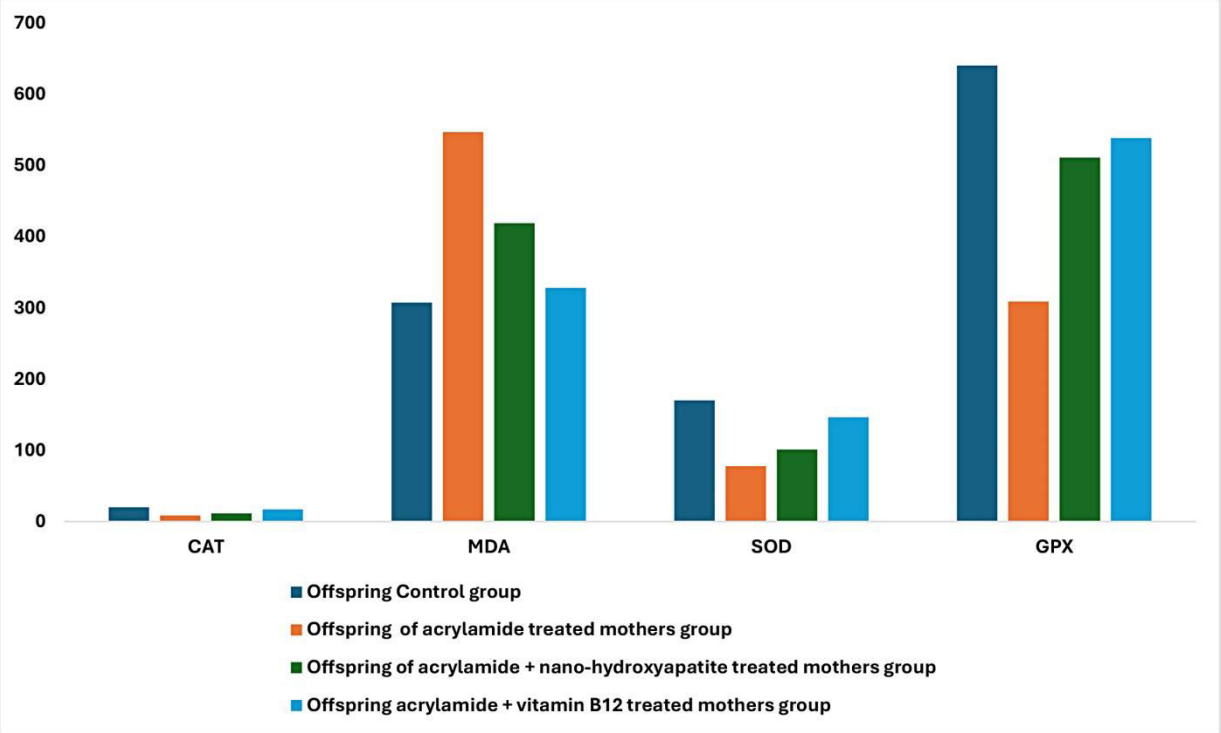

Fig.6. Variation in oxidant/antioxidant biomarkers in 21-day-old offspring from control and treated groups of pregnant rats

Light microscopic results

Histopathological examination of cerebellar sections from offspring at 15 days postnatal

Histopathological cerebellar investigation of the offspring control group showed that the external granular layer was normal. There was normal histological structure of purkinje cell layer that consisted of single raw of Purkinje cells that appeared oval well-defined and have an apical cone, pointing towards the surface of the cerebellar cortex. The molecular layer was well developed, markedly increased in thickness and contained few cells. The internal granular layer was crowded and had dense stained cells of variable shape and size **(Fig.7a)**. Offspring of the acrylamide treated mothers group showed decreased thickness of the external granular layer in comparison with the control group. There were deformed, shrunken and deep stained Purkinje cells. In addition, necrosis and nuclear pyknosis with hemorrhage and extravagated RBCs in white matter were observed. There was a sever edema in the inner granular layer **(Fig.7b)**. Offspring of acrylamide+nano-hydroxyapatite treated mothers group showed that the external granular layer was thick. Some Purkinje cells appeared normal with vesicular nuclei, while others appeared necrotic with homogenous pinkish acidophilic cytoplasm. The granular cell layer appeared mature with dense populated granule cells, **(Fig.7c)**. Offspring of acrylamide+vitamin B12 treated mothers group showed that the external granular layer was normal. Most Purkinje cells improved and appeared similar to the control. Some cells appeared degenerated with small nuclear pyknosis. There was an increase in the density of granular cell layer. There was no edema or

heamorrhage **(Fig.7d)**.

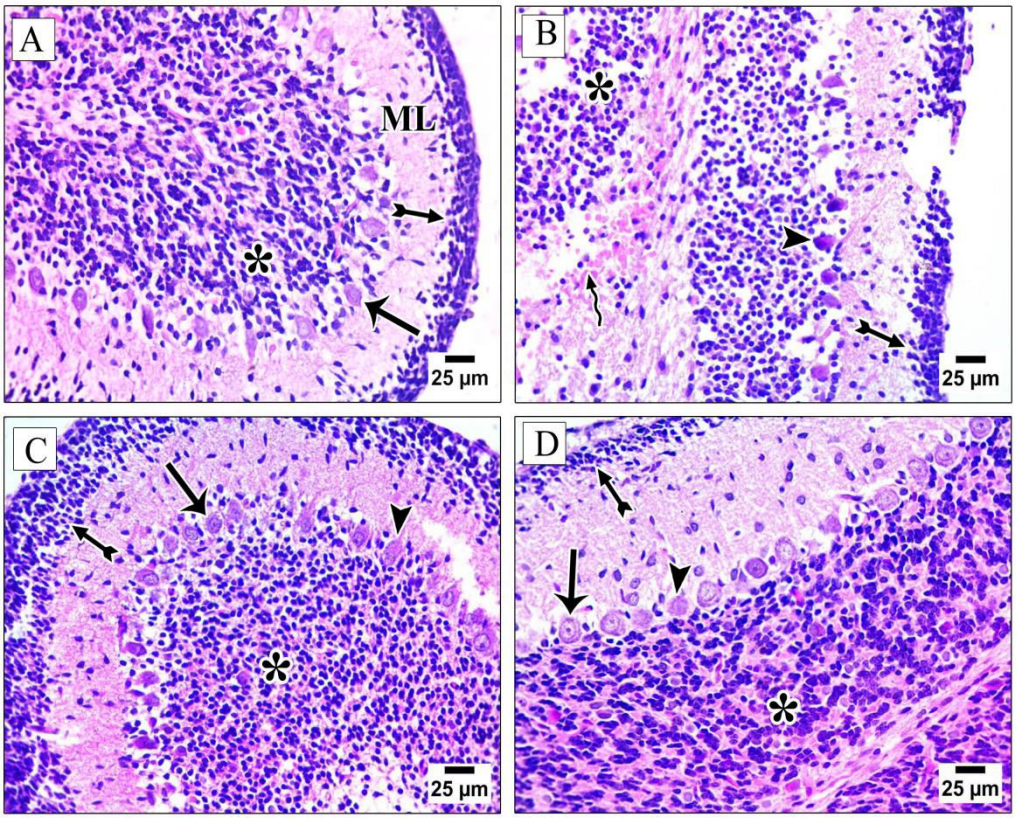

Fig. 7. Photomicrograph of the histopathological findings of the cerebellum of the studied groups of H&E stained tissue sections using light microscopy (X200) from offspring at 15 days postnatal. **(A)** Offspring control group: external granular layer (tailed arrow), normal purkinje cell (black arrow), molecular layer (ML), internal granular layer (asterisk). **(B)** Offspring of acrylamide treated mothers group: external granular layer (tailed arrow), necrotic purkinje cells (head arrow), hemorrhage (wavy arrow), inner granular layer edema (asterisk). **(C)** Offspring of acrylamide + nano-hydroxyapatite treated mothers group: external granular layer (tailed arrow), normal purkinje cells (black arrow), necrotic purkinje cells (head arrow), and normal granular cell layer (asterisk). **(D)** Offspring of acrylamide + vitamin B12 treated mothers group: external granular layer (tailed arrow), normal Purkinje cells (black arrow), pyknotic Purkinje cells (head arrow), and granular cell layer (asterisk).

Histopathological examination of cerebellar sections from offspring at 21 days postnatal

Histopathological cerebellar investigation of the offspring control group showed that the outer layer was the molecular layer that consisted mainly of fibers and few cells. Purkinje cell layer appeared with normal histological structure consists of one row of cells that were oval in shape with an apical dendrite. The granular layer appeared mature with dense stained cells of variable shape and size with cerebellar islands in between **(Fig.8a).** Offspring of the acrylamide treated mothers group showed that the Purkinje cells appeared necrotic with homogenous pinkish acidophilic cytoplasm and codensated nuclei. There was vacuolations in white matter **(Fig. 8b)**. Offspring of the acrylamide + nano-hydroxyapatite treated mothers group showed that normal Purhinje cells arranged in single row were observed. There were some Purkinje cells were necrotic with homogenous pinkish acidophilic cytoplasm was noticed. The granular layer contained granule cells oval or rounded in shape **(Fig.8c)**. Offspring of the acrylamide + vitamin B12 treated mothers group showed normal Purkinje cells. There was focus of small nuclear pyknosis

and normal density of granular cell layer was observed. No edema or hemorrhage was noticed **(Fig. 8d)**.

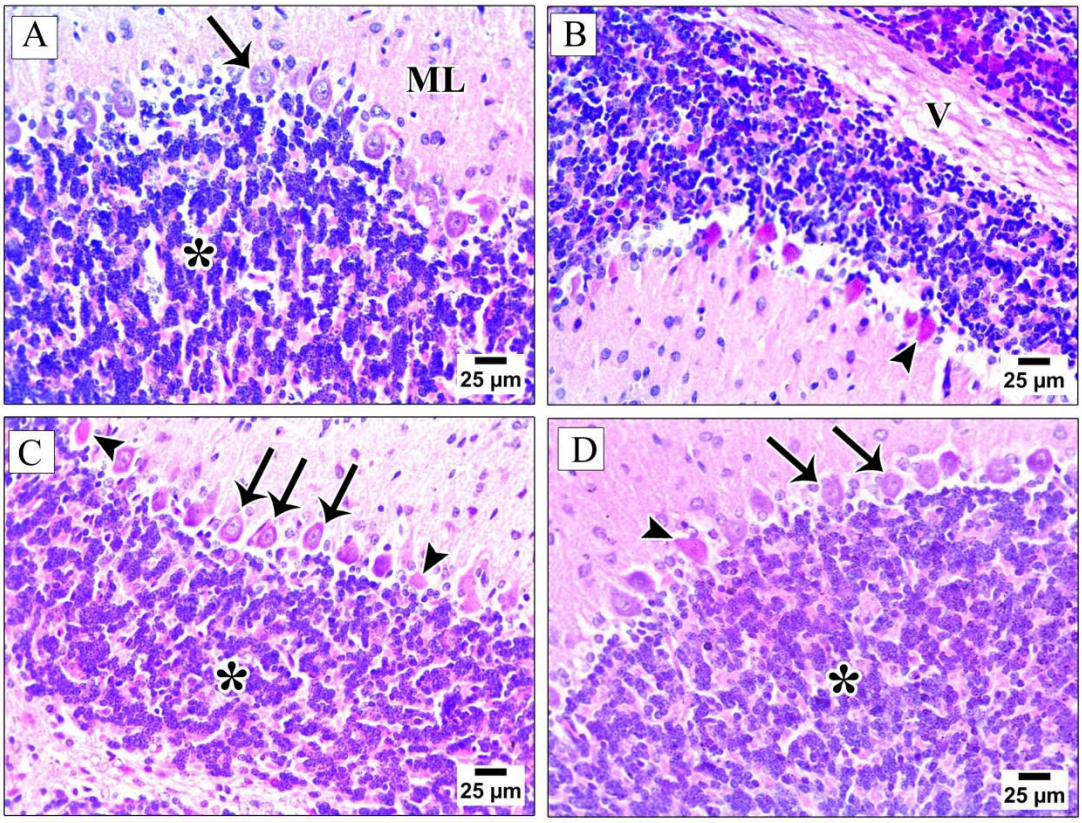

Fig. 8. Photomicrograph of the histopathological findings of the cerebellum of the studied groups of H&E stained tissue sections using light microscopy (X200) from offspring at 21 days postnatal. **(A)** Offspring control group: molecular layer (ML), normal purkinje cell (black arrow), granular layer (asterisk). **(B)** Offspring of Acrylamide treated mothers group: necrotic purkinje cells (head arrow), vacuolations (**V**). **(C)** Offspring of acrylamide + nano-hydroxyapatite treated mothers group: normal purkinje cells (black arrow), necrotic purkinje cells (head arrow) and granular layer (asterisk). **(D)** Offspring of acrylamide + vitamin B12 treated mothers group: normal purkinje cells (black arrow), pyknotic purkinje cells (head arrow), normal granular cell layer (asterisk).

Examination of the semithin cerebellar sections from offspring at 15 days postnatal

Sections from offspring control group showed normal histological structure of the cerebellar cortex. The extrernal granular layer was normal. The Purkinje cells were oval in shape and contained a vesicular nucleus, prominent nucleolus and arranged in a single row. The Purkinje cells were surrounded by Bergman glial cells. The molecular layer contained mainly fibers and few cells. The granular layer consisted of granule cells with cerebellar islands in between **(Fig.9a)**. Offspring of the acrylamide treated mothers group showed vacuolations in the external granular layer. Some Purkinje cells were abnormal with ill-defined nucleus. There was focal loss of Purkinje cells in some areas. There was vacuolations in the molecular layer **(Fig. 9b)**. Offspring of acrylamide + nano-hydroxyapatite treated mothers group showed that the extrernal granular layer contained vacuolations. Some Purkinje cells were normal and arranged in one row. There were vacuolations in the molecular layer. The granular layer appeared normal **(Fig.9c)**. Offspring of the acrylamide + vitamin B12 treated mothers group showed that the external

granular layer appeared normal. Most of the Purkinje cells improved, appeared normal and contained a vesicular nucleus and a prominent nucleolus. There were vacuolations in the molecular layer. The granular layer appeared normal and consisted of granule cells with cerebellar islands in between **(Fig.9d).**

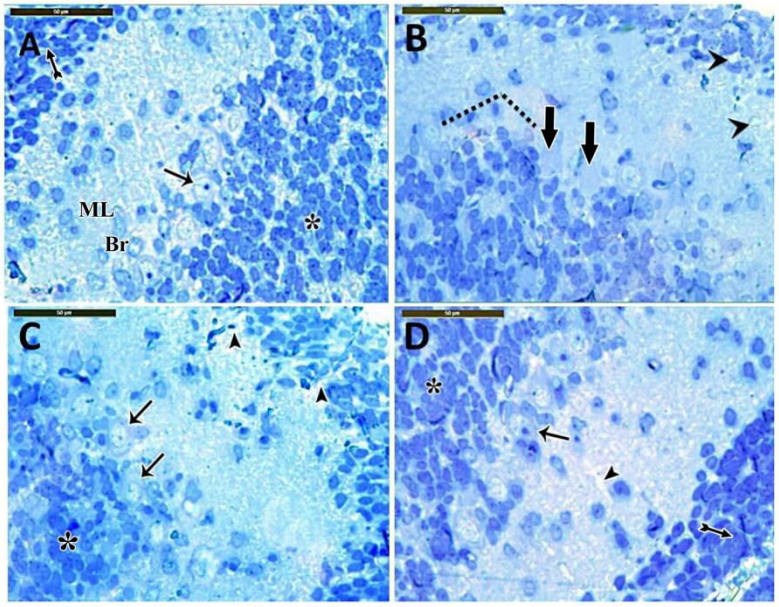

Fig.9: Photomicrograph of the histopathological findings of the cerebellum of the studied groups using Semihin sections stained with toluidine blue (X600) from offspring at 15 days postnatal. **(A)** Offspring control group: external granular layer (tailed arrow). Purkinje cells (black arrow), Bergman glial cells (Br), molecular layer (ML), granular layer (asterisk). **(B)** Offspring of acrylamide treated mothers group: external granular layer vacuolations (head arrow), abnormal Purkinje cells (thick arrow), focal loss of purkinje cells (dotted line), molecular layer vacuolations (head arrow). **(C)** Offspring of acrylamide + Nano-hydroxyapatite treated mothers group: external granular vacuolations (head arrow), normal Purkinje cells (black arrow), molecular layer vacuolations (head arrow), granular layer (asterisk). **(D)** Offspring of acrylamide + vitamin B12 treated mothers group: extrernal granular layer (tailed arrow), normal Purkinje cells (black arrow), molecular layer vacuolations (head arrow), granular layer (asterisk).

Examination of the semithin cerebellar sections from offspring at 21 days postnatal

Sections from offspring control group showed that the molecular layer contained mainly fibers and few cells. The Purkinje cell layer contained normal Purkinje cells with vesicular nucleus and a prominent nucleolus. The Purkinje cells surrounded by Bergman glial cells. The granular layer consisted of granule cells with cerebellar islands in between (**Fig.10a**). Offspring of the acrylamide treated mothers group showed abnormal Purkinje cells with dense stained cytoplasm and irregular nucleur membrane. Some Purkinje cells appeared shrunken with ill-defined nucleus. Perineuronal space was observed around the cells in the Purkinje cell layer. There were many vacuolations in the molecular layer (**Fig.10b**). Offspring of acrylamide + nano-hydroxyapatite treated mothers group showed some Purkinje cells were normal but some had abnormal shape and dense stained cytoplasm with ill-identified nucleus. There were many vacuolations in the molecular layer. The granular layer appeared normal and consisted of granule cells with cerebellar islands in between (**Fig.10c**). Offspring of the acrylamide + vitamin B12 treated mothers group showed most Purkinje cells improved,

appeared normal and contained a vesicular nucleus and a prominent nucleolus. Some cells have abnormal shape and dense stained cytoplasm with ill-identified nucleus. The granular layer appeared normal **(Fig.10d)**.

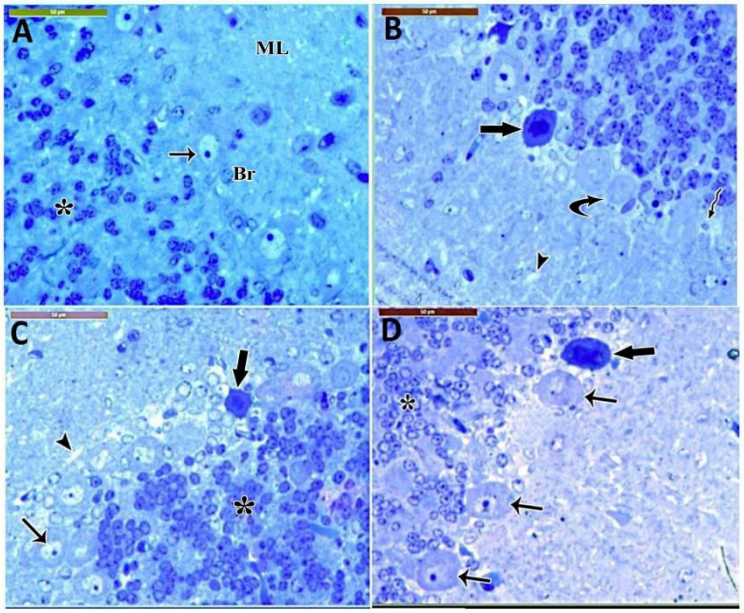

Figure 10: Photomicrograph of the histopathological findings of the cerebellum of the studied groups using Semihin sections stained with toluidine blue (X600) from offspring at 21 days postnatal. **(A)** Offspring control group: molecular layer (ML), normal Purkinjie cells (black arrow), Bergman glial cells (Br), granular layer (asterisk). **(B)** Offspring of acrylamide treated mothers group: abnormal Purkinje cells (thick arrow). shrunken Purkinje cells (curved arrow), perineuronal space (wavy arrow), molecular layer vacuolations (head arrow). **(C)** Offspring of acrylamide + Nano-hydroxyapatite treated mothers group: normal Purkinje cells (black arrow), abnormal Purkinje cells (thick arrow), molecular layer vacuolations (head arrow), granular layer (asterisk). **(D)** Offspring of acrylamide + vitamin B12 treated mothers group: normal Purkinje cells (black arrow), abnormal Purkinje cells (thick arrow), granular layer (asterisk).

Electron microscopic examinations

Examination of section of the cerebellum from offspring at 15 days postnatal (Molecular layer)

Offspring control group showed intact myelinated nerve fibers with no splitting or disruption **(Fig.11a)**. Offspring of the acrylamide treated mothers group showed disruption of the myelin sheath. There were vacuoles in the neuropil **(Fig. 11b)**. Offspring of the acrylamide + nano-hydroxyapatite treated mothers group showed intact myelinated nerve fibers. Some of the fibers showed split of their myelin sheath **(Fig.11c)**. Offspring of the acrylamide + vitamin B12 treated mothers group showed intact myelinated nerve fibers. Some of the fibers showed splitting of their myelin sheath. There were vacuoles in the neuropil **(Fig. 11d)**.

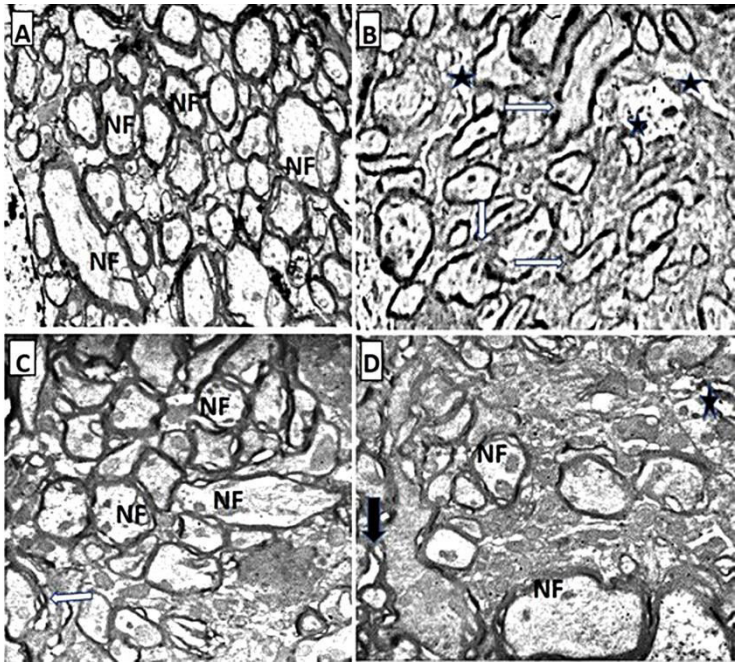

Fig.11. Transmission electron micrograph of cerebellar tissue in the molecular layer (X15000) from offspring at 15 days postnatal. **(A)** Offspring control group: intact nerve fibers (NF). **(B)** Offspring of acrylamide treated mother's group: disruption of nerve fibers (white arrow), vacuoles (star).**(C)** Offspring of acrylamide + nano-hydroxyapatite treated mothers group: intact nerve fibers (NF), splitting of myelin sheath (white arrow). **(D)** Offspring of acrylamide + vitamin B12 treated mothers group: intact nerve fibers (NF), splitting of myelin sheath (black arrow), vacuoles (star).

Examination of section of the cerebellum from offspring at 15 days postnatal (granular layer)

Offspring control group showed Granule cells having heterochromatic nuclei and thin rim of cytoplasm. Notice, a Golgi cell **(Fig.12a)**. Offspring of the acrylamide treated mothers group showed that the granular cell had some area of focal degenerations. Some granule cells appeared shrunken. There were some cells with irregular nuclear membrane **(Fig.12b)**. Offspring of the acrylamide + nano-hydroxyapatite treated mothers group showed that some Granule cells appeared normal (oval or rounded cells with heterochromatin), while some cells had irregular nuclear membrane. Some fibers showed splitting of the myelin sheath **(Fig.12c)**. Offspring of the acrylamide + vitamin B12 treated mothers group showed that granule cells appeared more or less normal. Some cells were shrunken. The surrounding neuropil contained many vacuoles **(Fig.12d)**.

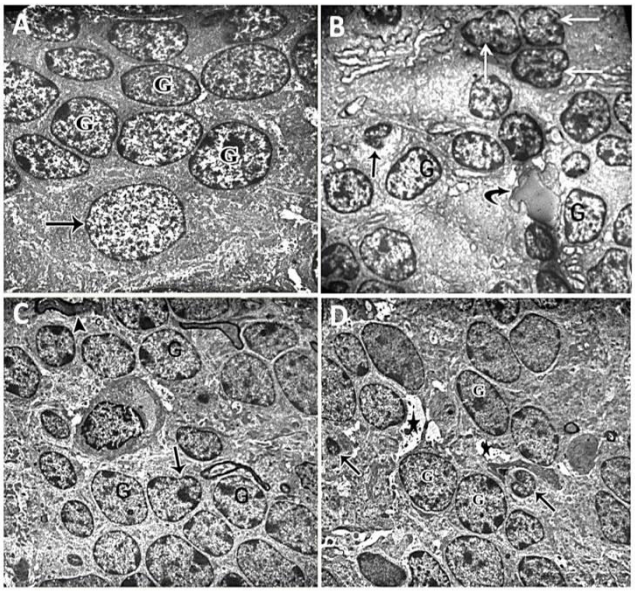

Fig.12. Transmission electron micrograph of cerebellar tissue in the granular layer (X15000) from offspring at 15 days postnatal. **(A)** Offspring control group: normal granule cells (G), Golgi cell (black arrow)**. (B)** Offspring of acrylamide treated mothers group: granular cell (G), focal degenerations (curved arrow), shrunken granule cells (black arrow), irregular nuclear membrane (white arrow). **(C)** Offspring of acrylamide + nano-hydroxyapatite treated mothers group: normal granule cells (G) irregular nuclear membrane (black arrow), splitting of myelin sheath (head arrow). **(D**) Offspring of acrylamide + vitamin B12 treated mothers group: normal granule cells (G), shrunken granule cells (black arrow), vacuoles (star).

Examination of section of the cerebellum from offspring at 21 days postnatal (Molecular layer)

Offspring control group showed intact myelinated nerve fibers **(Fig.13a)**. Offspring of the acrylamide treated mothers group showed splitting of the myelin sheath (**Fig.13b)**. Offspring of the acrylamide + nano-hydroxyapatite treated mothers group showed intact myelinated nerve fibers. Some of the fibers showed split of their myelin sheath. Presence of vacuoles were notice **(Fig.13c)**. Offspring of the acrylamide + vitamin B12 treated mothers group showed intact myelinated nerve fibers and also vacuoles were observed in the neuropil **(Fig. 13d)**.

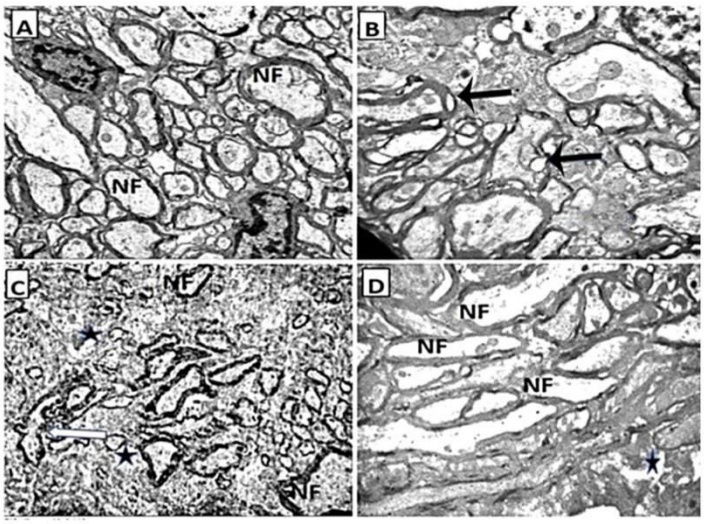

Fig.13. Transmission electron micrograph of cerebellar tissue in the molecular layer (X15000) from offspring at 21 days postnatal. **(A)** Offspring control group: intact nerve fibers (NF). **(B)** Offspring of acrylamide treated mothers group: splitting of myelin sheath (black arrow). **(C)** Offspring of

acrylamide + nano-hydroxyapatite treated mothers group: intact nerve fibers (NF), splitting of myelin sheath (white arrow), vacuoles (star). **(D**) Offspring of acrylamide + vitamin B12 treated mothers group: intact nerve fibers (NF), vacuoles (star).

Examination of section of the cerebellum from offspring at 21 days postnatal (granular layer)

Offspring control group showed the normal structure of granular cells. They were oval or rounded in shape. Their nuclei were large with condensed chromatin and a thin rim of cytoplasm **(Fig.14a)**. Offspring of the acrylamide treated mothers group showed some granule cells with irregular nuclear membrane and others were shrunken. Some myelin fibers showed splitting at myelin sheath **(Fig.14b)**. Offspring of the acrylamide + nano-hydroxyapatite treated mothers group showed granular cells. Some granule cells appeared normal in size, while others had irregular nuclear membrane. There were abnormal cells appeared with irregular nuclear membrane and condensed chromatin and others were shrunken **(Fig.14c)**. Offspring of the acrylamide + vitamin B12 treated mothers group showed some granule cells appeared normal in size (oval or rounded cells with heterochromatin). The others appeared with irregularity in the nuclear membrane. There were many vacuoles in the surrounding neuropil **(Fig.14d)**.

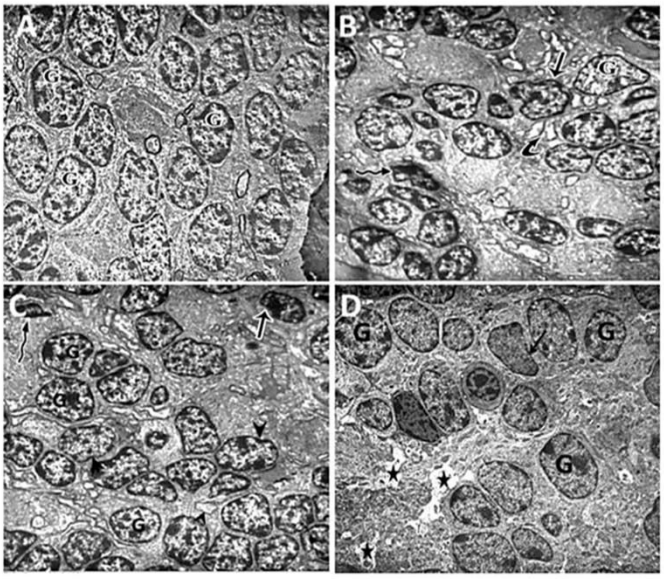

Fig.14. Transmission electron micrograph of cerebellar tissue in the granular layer (X15000) from offspring at 21 days postnatal. **(A)** Offspring control group: normal granular cells (G). **(B)** Offspring of acrylamide treated mothers group: irregular nuclear membrane (black arrow), shrunken granular cells (wavy arrow), splitting at myelin sheath (curved arrow). **(C**) Offspring of acrylamide + nano-hydroxyapatite treated mothers group: normal granular cells (G). irregular nuclear membrane (head arrow), condensed chromatin (black arrow), shrunken granular cells (wavy arrow). **(D)** Offspring of acrylamide + vitamin B12 treated mothers group: normal granule cells (G), irregular nuclear membrane (black arrow), vacuoles (star).

Discussion

In the current study, statistical analysis of the histopathological investigation of the cerebellum of the produced offspring revealed that all studied parameter such as Purkinje cell count; granular layer thickness, Purkinje layer thickness, and molecular layer thickness were significantly reduced in the ACR group compared with the control one. Similar results were reported by **Abdullah et al. (2023)** who announced that severe cerebellar damage were observed

following subchronic acrylamide exposure in adult rats such as notable loss of Purkinje cells and thinning of the granular layer, echoing our developmental findings. Acrylamide and their metabolites pass easily through the placenta due to their solubility in water and are distributed in many fetal tissues during pregnancy **(Sorgel et al., 2002).**

Our results revealed that acrylamide exposure induced severe histopathological damage in the cerebellum, affecting not only Purkinje cell survival but also the structural integrity of the granular, Purkinje, and molecular layers. The reduction in Purkinje cells, which are essential for cerebellar output and motor coordination, suggests significant neuronal loss. The observed thinning of all cerebellar layers reflects impaired neurogenesis and synaptogenesis, and possibly degeneration of glial and neuronal support elements. This supports the hypothesis that acrylamide disrupts developmental processes in the brain, including neuronal maturation and differentiation, as previously described by **Wang et al. (2021).**

In the current trial, Nano-Hydroxyapatite administration in combination with ACR (acrylamide+nano-hydroxyapatite mother treated group) provided partial neuroprotection, improving all parameters significantly compared to acrylamide group, though values remained below control levels. Our results are in agreement with **Yadav et al. (2024)** who noted that Nano-hydroxyapatite may contribute neuronal stability by maintaining calcium homeostasis and exerting antioxidant effects. In addition, **Huang et al. (2023)** found that tissue damage scores in acrylamide-exposed rats were the highest and significantly reduced after administration of HA and/or Vit.B12, with the most robust protective effect was recorded for Vit.B12.

In the current study, the protective role of nano-hydroxyapatite was moderate compared to Vitamin B12 that was administrated in combination with ACR (acrylamide + Vitamin B12 mother treated group), which demonstrated superior efficacy across all examined parameters. These results are consistent with **Mustafa and Hussein (2016)** who reported that co-administration of allicin and Vit.B12 led to modest improvements in Purkinje and granular cell layers in acrylamide-exposed rats. Besides, **Cuyubamba et al. (2025)** stated that Vit.B12 lowers homocysteine levels, reducing neuroinflammation and oxidative stress-two key mechanisms in acrylamide-induced neurotoxicity. Moreover**, Yadav et al. (2024)** highlighted the role of Vitamin B12 in DNA synthesis, myelination, methylation reactions, and neuronal energy metabolism.

The preservation of Purkinje cells and cortical thickness in the acrylamide + Vitamin B12 group in the current trial may be attributed to the strong neuroprotective, anti-apoptotic, and neuroregenerative properties of Vit.B12. Moreover, recent research has shown that Vit.B12 has a strong protective effect against toxicity caused by the long-term use of high doses of therapeutic drugs such as ivermectin, further confirming the potent protective properties of Vitamin B12 **(Asmaa et al. 2025).**

In our study, at 15 and 21 days postnatally, histological analysis showed a significant reduction in all cerebellar parameters in the ACR group compared to controls. At that days, Purkinje cell count, granular layer thickness, Purkinje layer thickness, and molecular layer thickness were all significantly

decreased ($P < 0.0001$).

In agreement with our study, **Liu et al. (2021)** demonstrated that subchronic ACR exposure induced cerebellar neuronal lesions in rats. Histologically, hematoxylin-eosin staining revealed mineralized Purkinje cells with nuclear condensation, pyknosis, and chromatolysis. Nissl staining showed Purkinje cell pyknosis, reduced Nissl body intensity, and structural damage. So, as in our study, these structural abnormalities were reflected quantitatively by a significant reduction in Purkinje cell count and decreased Purkinje layer thickness, confirming similar neurotoxic effects of ACR on cerebellar architecture.

Similarly, **Amin et al. (2019)** reported that acrylamide exposure in pregnant albino rats during gestation (prenatal group) and gestation plus lactation (postnatal group) led to marked cerebellar degeneration in offspring, worsening with longer exposure. Control offsprings exhibited normal cerebellar architecture while treated groups showed progressive histological damage across postnatal days of 14 and 21, including thinning and exfoliation of the external granular layer, vacuolated molecular layer, degenerated Purkinje cells with karyolysis and loss of axons, and disorganized internal granular layer with vacuolated or aggregated granule cells.

In the current study, administration of Vit.B12 in combination with ACR improved the histological outcomes observed on postnatal days 15 and 21, with the ACR + Vitamin B12 group showing cerebellar parameters comparable to those of the control group. Supporting our findings, **Eltony (2016)** study used male Wistar rats to evaluate the protective effect of vitamin B complex against STZ-induced diabetic cerebellar damage. It was noted that in vitamin B complex-treated rats, granule cells and cerebellar glomeruli appeared normal. Purkinje neurons were preserved, with euchromatic nuclei and cytoplasm containing well-developed organelles, indicating protective effects similar to those observed in our vitamin-treated group.

Various studies have investigated the oxidant/antioxidant profile and used it as a tool to monitor the development of different diseases **(Amin et al. 2020; Amin et al. 2021; Amin et al. 2023b; El-Sawy et al. 2023)**. Others have highlighted its role in drug or toxicant-induced toxicity **(Toghan et al. 2022; Allam et al. 2025)**, while some have illustrated its importance as a key factor in the treatment process **(Awadalla et al. 2025)**.

Our study showed that acrylamide exposure in offspring rats induced significant oxidative stress, reflected by a marked reduction in CAT, SOD and GP_X activities, alongside a significant increase in MDA levels. Treatment with either Nano-hydroxyapatite or Vit.B12 significantly restored antioxidant enzyme activities such as CAT, SOD, and GPX levels and lowering MDA, indicating superior neuroprotective efficacy compared to Nano-hydroxyapatite.

These findings align with **Abbas et al. (2019)** who demonstrated that nano-hydroxyapatite reduced oxidative markers and improved brain histology in aluminum-induced neurotoxicity. **Xu et al. (2021)** found that hydroxyapatite preserved synaptic function and promoted axonal regeneration in cerebral ischemia models.

Furthermore, **Batool et al. (2022)** reported that adenosylcobalamin, a derivative of vitamin B12, offered significant protection against DEHP-induced

oxidative damage in rats by restoring antioxidant enzyme levels and reducing lipid peroxidation. Vitamin B12 superior effects are also consistent with **Wu et al. (2019),** who reported that mecobalamin reduced neuronal apoptosis, improved remyelination, and enhanced neurological function in traumatic brain injury models. Similarly, **Suryavanshi et al. (2024)** showed that vitamin B12 facilitated neuronal survival and functional recovery in peripheral nerve injury, underlining its potent neuro-regenerative and antioxidant properties.

Our study also revealed that with age, antioxidant defenses naturally improved. The ACR-exposed rats treated with HA or Vit.B12 in this study, maturation-dependent antioxidant restoration was observed. From 15 to 21 days postnatal of the produced offspring, CAT, SOD, and GPX activities significantly increased, while MDA levels decreased. Vitamin B12 consistently outperformed hydroxyapatite, showing earlier and more effective normalization of oxidative markers. These age-related trends are supported by findings from **Ryan et al. (2008)** and **Aliahmat et al. (2012)** who reported increased antioxidant enzyme activities and decreased lipid peroxidation markers with development in various tissues and species.

Conclusion

Our study demonstrates that acrylamide exposure to the mother during pregnancy and nursing resulted in production of offspring suffered from significant cerebellar histopathological damage and oxidative stress. Histopathological investigation of the cerebellum of the produced offspring showed reduced Purkinje cell count and cortical layer thickness along with decreased serum antioxidant enzyme activities (CAT, SOD, GPX) and elevated MDA levels ($P < 0.0001$). Co-treatment with nano-hydroxyapatite partially ameliorated these effects showing significant recovery but with but limited degree. In contrast, vitamin B12 demonstrated superior neuroprotective efficacy, significantly restoring of the cerebellum histological architecture and significant improvement of serum oxidant/antioxidant parameters with MDA levels almost normalized by day 21. All of these indicating a potent antioxidant and neuroprotective role of Vit.B12 against acrylamide-induced neurotoxicity.

References

- **Abbas OA, Ibrahim IG, Ismail AE. (2019).** Therapeutic effects of Nano-HAp in a rat model of $AlCl_3$-induced neurotoxicity. Iranian Journal of Pharmaceutical Research, 18(3): 1309–1322.
- **Abdullah AM, AL Badawi MH, Abdelhady AA. (2023).** The protective role of selenium against acrylamide-induced cerebellar neurotoxicity in adult male albino rats. Egyptian Journal of Histology, 1(1): 1-12.
- **Aebi H. (1984).** Catalase in vitro. Methods in Enzymology, 105(1): 121–126.
- **Ahmed R, El-Nahas SA, Mohamed A. (2022).** Structural and morphological features of hydroxyapatite nanoparticles from different calcium resources. Aswan University Journal of Environmental Studies, 3(3), 313-323.
- **Aliahmat NS, Noor MRM, Yusof WJW, Makpol S, Ngah WZW, Yusof YAM. (2012).** Antioxidant enzyme activity and malondialdehyde levels can be modulated by Piper betle, tocotrienol-rich fraction and Chlorella vulgaris in aging C57BL/6 mice. Clinics, 67: 1447–1454.

- **Allam M, Amin YA, Fouad SS, Ali RA, Fawy MA, Ahmed MA-EB, Toghan R, Ali LA. (2025).** Mesenchymal stem cells reduce the genotoxic effect of lead acetate in the testis of male rats and induce testicular cellular proliferation indicated by 16S rRNA sequence, increase the proliferation marker Ki-67 and a reduction in the apoptosis marker caspase-3. Biological Research 58 (1):1-15.
- **Amin WES, Hegab AS, Ibrahim AAS, Mokhtar HE. (2019).** Effect of acrylamide on development of cerebellum in albino rat. Egyptian Journal of Histology, 42(4): 798–814.
- **Amin YA, Abdelaziz SG, Said AH. (2023a)**. Treatment of postpartum endometritis induced by multidrug-resistant bacterial infection in dairy cattle by green synthesized zinc oxide nanoparticles and in vivo evaluation of its broad spectrum antimicrobial activity in cow uteri. Research in veterinary science 165:105074
- **Amin YA, Ali RA, Fouad SS, Ibrahim RM. (2021)**. The deleterious effect of postpartum pyometra on the reproductive indices, the metabolic profile, and oxidant/antioxidant parameters of dairy cows. Veterinary World 14 (2):329
- **Amin YA, Noseer EA, Fouad SS, Ali RA, Mahmoud HY. (2020)**. Changes of reproductive indices of the testis due to Trypanosoma evansi infection in dromedary bulls (Camelus dromedarius): semen picture, hormonal profile, histopathology, oxidative parameters, and hematobiochemical profile. Journal of Advanced Veterinary and Animal Research 7 (3):537
- **Amin YA, Omran GA, Fouad SS, Fawy MA, Ibrahim RM, Khalifa FA, Ali RA. (2023b)**. Abortion associated with postpartum opportunistic bacterial invasion reduces fertility and induces disturbances of reproductive hormones, hematological profile, and oxidant/antioxidant profiles in dairy cows. Journal of advanced veterinary and animal research 10 (4):654
- **Asmaa M. Mosa, Rana A. Ali, Seham A. Mobarak, Zeinab A. Mar'ie, and Yahia A. Amin. (2025)**. Impact of chronic ivermectin toxicity on some blood parameters and liver and kidney histoarchitectonics of adult albino rats: evaluation of the role of folic acid and vitamin b12 as new treatment modalities, Cell and Tissue Biology, 19(5) 470–480.
- **Aguwa US, Eze CE, Obinwa BN, Okeke SN, Onwuelingo SF, Okonkwo DI, Ogbuokiri DK, Agulanna A, Obiesie I, Umezulike A. (2020).**Comparing the effect of methods of rat euthanasia on the brain of Wistar rats: Cervical dislocation, chloroform inhalation, diethyl ether inhalation and formalin inhalation. Journal of Advances in Medical and Biomedical Research 32(17):8-16.
- **Awadalla EA, Amin YA, Ali RA, Gbr SA, Gelany WI, Nour AH. (2025)**. Co-treatment of β-carotene with acetamiprid provides protection against acetamiprid induced hepatic and renal toxicity via modulation of the antioxidant system. BMC Pharmacology and Toxicology 26 (1):1-15
- **Awais M, Aizaz A, Nazneen A, Bhatti QUA, Akhtar M, Wadood A, et al. (2022).** A review on the recent advancements on therapeutic effects of ions in the physiological

environments. Prosthesis, 4(2): 263–316.

- **Ayache J, Beaunier L, Boumend L, Ehret G. (2010).** Sample preparation handbook for transmission electron microscopy. Sample Preparation Handbook for Transmission Electron Microscopy, 423–4821.
- **Baltrusch S. (2021).** The role of neurotropic B vitamins in nerve regeneration. BioMed Research International, 2021(1): 9968228.
- **Bancroft J, Gamble M. (2008).** Theory and practice of histological techniques. Theory and Practice of Histological Techniques, 400–421.
- **Batool S, Batool S, Shameem S, Batool T, Batool S. (2022).** Effects of dibutyl phthalate and di(2-ethylhexyl) phthalate on hepatic structure and function of adult male mice. Toxicology and Industrial Health, 38(8): 470–480.
- **Behairy A, El-Sharkawy NI, Saber TM, Soliman MM, Metwally, MM, Abd El-Rahman GI, Abd-Elhakim YM, El Deib MM. (2020).** The Modulatory Role of Vitamin C in Boldenone Undecylenate Induced Testicular Oxidative Damage and Androgen Receptor Dysregulation in Adult Male Rats. Antioxidants (Basel, Switzerland), 9 (11): 1053.
- **Calderón-Ospina CA, Nava-Mesa MO. (2020).** B Vitamins in the nervous system: Current knowledge of the biochemical modes of action and synergies of thiamine, pyridoxine, and cobalamin. CNS Neuroscience & Therapeutics, 26(1): 5–13.
- **Celik I, Seker M, Salbacak A. (2018).** Histological and histomorphometric studies on the cerebellar cortex and silver stained nucleolus organizer regions of Purkinje neurons in chronic morphine-treated rats. Veterinarski Arhives, 88(1):75-88.
- **Cuyubamba O, Braga CP, Swift D, Stickney JT, Viel C. (2025).** The combination of neurotropic vitamins B1, B6, and B12 enhances neural cell maturation and connectivity superior to single B vitamins. Cells, 14(7): 1-24.
- **Ehmedah A. (2024).** Effect of vitamin B complex therapy on process of neuroinflammation and regeneration of rat peripheral nerve after injury. University of Belgrade.
- **El-Sawy SA, Amin YA, El-Naggar SA, Abdelsadik A. (2023)**. Artemisia annua L.(Sweet wormwood) leaf extract attenuates high-fat diet-induced testicular dysfunctions and improves spermatogenesis in obese rats. Journal of ethnopharmacology 313:116528.
- **Eltony SA. (2016).** Histological study on the protective role of vitamin B complex on the cerebellum of diabetic rat. Tissue Cell, 48(4): 283–296.
- **Hafez AI, Hafez F, Khedr M, Ibrahim O, Sabry R, Abdel-Wahhab MA, et al. (2012).**Safety evaluation of needle-like hydroxyapatite nanoparticles in female rats. Egyptian Pharmaceutical Journal, 11(2), 67-72.
- **Huang Z, Wang S, Yang Y, Lou J, Liu Z, Liu Z, et al. (2023).** Mitochondrial dysfunction promotes the necroptosis of Purkinje cells in the cerebellum of acrylamide-exposed rats. Food and Chemical Toxicology, 171(1): 1-12.
- **Kubiak-Mihkelsoo Z, Kostrzębska A, Błaszczyszyn A, Pitułaj A, Dominiak M, Gedrange T, et al. (2025).** Ionic doping of hydroxyapatite for bone

regeneration: Advances in structure and properties over two decades—A narrative review. Applied Sciences, 15(3): 1108.

- **Liu M, Zhou G, Song W, Li P, Liu H, Niu X, et al. (2012).** Effect of nano-hydroxyapatite on the axonal guidance growth of rat cortical neurons. Nanoscale, 4(10): 3201–3207.
- **Liu Y, Yan D, Wang Y, Zhang X, Wang N, Jiao Y, et al. (2021).** Subchronic exposure to acrylamide caused behaviour disorders and related pathological and molecular changes in rat cerebellum. Toxicology Letters, 340(1): 23–32.
- **Malla KP, Malla B, Pandit R, Pokharel S, Yadav RJ, Adhikari R, et al. (2024).** Acute Oral Toxicity Analysis of Nano-Hydroxyapatite-Gelatin Suspension in Albino Wistar Rats. Journal of Nepal Chemical Society, 44(1), 78-90.
- **Mathew AR, Di Matteo G, La Rosa P, Barbati SA, Mannina L, Moreno S, et al. (2024).** Vitamin B12 deficiency and the nervous system: Beyond metabolic decompensation—comparing biological models and gaining new insights into molecular and cellular mechanisms. International Journal of Molecular Sciences, 25(1): 590.
- **Moawad R, Abd El Fattah E, Ramadan R. (2019)**. Postnatal Effect Of Acrylamide On Rat Renal Cortex And The Protective Effect Of Ginger (Zingiber Officinale Roscoe). Egyptian Journal of Histology, 42(1): 51-63.
- **Moosavirad SA, Rabbani M, Sharifzadeh M, Hosseini-Sharifabad A. (2016).** Protective effect of vitamin C, vitamin B12 and omega-3 on lead-induced memory impairment in rat. Research in Pharmaceutical Sciences, 11(5), 390-396.
- **Mustafa HN, Hussein A. (2016).** Does allicin combined with vitamin B-complex have superior potentials than alpha-tocopherol alone in ameliorating lead acetate-induced Purkinje cell alterations in rats? An immunohistochemical and ultrastructural study. Folia Morphologica, 75(1): 76–86.
- **Nishikimi M, Rao NA, Yagi K**. **(1972).** The occurrence of superoxide anion in the reaction of reduced phenazine methosulfate and molecular oxygen. Biochem Biophys Res Commun, 46(2): 849–854.
- **Ognio, E., Lapide, M., Ottone, M., Mandys, V., Peterka, M., Parodi, B., & Viale, M. (2003**). Embryo-lethal and teratogenic effect of the new platinum compound DPR in pregnant mice. Archives of toxicology, 77(10), 584-590.
- **Paglia DE, Valentine WN. (1967).** Studies on the quantitative and qualitative characterization of erythrocyte glutathione peroxidase. J Lab Clin Med, 70(1): 158–169.
- **Peivasteh-Roudsari L, Karami M, Barzegar-Bafrouei R, Samiee S, Karami H, Tajdar-Oranj B, et al. (2024).** Toxicity, metabolism, and mitigation strategies of acrylamide: a comprehensive review. International Journal of Environmental Health Research, 34(1): 1–29.
- **Ruiz-Larrea MB, Leal AM, Liza M, Lacort M, de Groot H. (1994).** Antioxidant effects of estradiol and 2-hydroxyestradiol on iron-induced lipid peroxidation of rat liver microsomes. Steroids, 59(6): 383–388.
- **Ryan MJ, Dudash HJ, Docherty M, Geronilla KB, Baker BA, Haff GG, et al. (2008).** Aging-dependent regulation of antioxidant enzymes and redox status in chronically loaded rat dorsiflexor

muscles. Journal of Gerontology A: Biological Sciences and Medical Sciences, 63(10): 1015–1025.

- **Sorgel F, Weissenbacher R, Kinzig-Schippers M, Hofmann A, Illauer M, Skott ALandersdorfer C. (2002).** Acrylamide increased concentrations in homemade food and first evidence of its variableabsorption from food, variable metabolism and placental and breast milk transfer in humans. Chemotherapy, 48: 267-274.
- **Suryavanshi U, Angadi KK, Reddy VS, Reddy GB. (2024).** Neuroprotective role of vitamin B_{12} in streptozotocin-induced type 1 diabetic rats. Chemico-Biological Interactions, 387: 110823.
- **Toghan R, Amin YA, Ali RA, Fouad SS, Ahmed MA-EB, Saleh SM. (2022).** Protective effects of Folic acid against reproductive, hematological, hepatic, and renal toxicity induced by Acetamiprid in male Albino rats. Toxicology 469:153115
- **Wang Y, Duan L, Zhang X, Jiao Y, Liu Y, Dai L, Yan H. (2021).** Effect of long-term exposure to acrylamide on endoplasmic reticulum stress and autophagy in rat cerebellum. Ecotoxicology and Environmental Safety, 224(1): 1-9.
- **Wu F, Xu K, Liu L, Zhang K, Xia L, Zhang M, et al. (2019).** Vitamin B12 enhances nerve repair and improves functional recovery after traumatic brain injury by inhibiting ER stress-induced neuron injury. Frontiers in Pharmacology, 10: 406.
- **Xu J, Wang C, Xu P. (2021).** Effects of hydroxyapatite extract on rats with transient ischemia: Long-term potentiation and axon regeneration. Experimental and Therapeutic Medicine, 22(6): 1486.
- **Yadav P, Nasir F, Sivanandam TM. (2024).** Neuroprotective effect of vitamin B12 supplementation on cognitive functions and neuronal morphology at different time intervals after traumatic brain injury in male Swiss albino mice. Neurochemistry International, 180(1): 1-15.
- **Yan F, Wang L, Zhao L, Wang C, Lu Q, Liu R. (2023).** Acrylamide in food: Occurrence, metabolism, molecular toxicity mechanism and detoxification by phytochemicals. Food and Chemical Toxicology, 175: 113696.
- **Zhao M, Zhang B, Deng L. (2022).** The mechanism of acrylamide-induced neurotoxicity: current status and future perspectives. Frontiers in Nutrition, 9(1), e859189.
- **ZiaZ. (2022).** Synthesis and characterisation of low-cost biopolymeric/mineral composite systems and evaluation of their potential application for heavy metal removal (Doctoral dissertation, The U University of Waikato), 1(1): 1-476.